

## Evolution of Proto-Neutron Stars with Quarks

José A. Pons, Andrew W. Steiner, Madappa Prakash, and James M. Lattimer

*Department of Physics and Astronomy, SUNY at Stony Brook, Stony Brook, New York 11794-3800*

(Received 1 February 2001)

Neutrino fluxes from proto-neutron stars with and without quarks are studied. Observable differences become apparent after 10–20 s of evolution. Sufficiently massive stars containing negatively charged, strongly interacting, particles collapse to black holes during the first minute of evolution. Since the neutrino flux vanishes when a black hole forms, this is the most obvious signal that quarks (or other types of strange matter) have appeared. The metastability time scales for stars with quarks are intermediate between those containing hyperons and kaon condensates.

DOI: 10.1103/PhysRevLett.86.5223

PACS numbers: 97.60.Jd, 12.38.Mh, 21.65.+f, 26.60.+c

A proto-neutron star (PNS) is born following the gravitational collapse of the core of a massive star, in conjunction with a successful supernova explosion. During the first tens of seconds of evolution, nearly all ( $\sim 99\%$ ) of the remnant's binding energy is radiated away in neutrinos of all flavors [1]. The  $\nu$  luminosities and the evolutionary time scale are controlled by several factors, such as the total mass of the PNS and the  $\nu$  opacity at supranuclear density, which depends on the composition and equation of state (EOS). One of the chief objectives in modeling PNSs is to infer their internal compositions from  $\nu$  signals detected from future supernovae by detectors such as Super-K, SNO, and others under consideration, including UNO [2].

In their landmark paper, Collins and Perry [3] noted that the superdense matter in neutron star cores might consist of weakly interacting quarks rather than of hadrons, due to the asymptotic freedom of QCD. The appearance of quarks causes a softening of the EOS which leads to a reduction of the maximum mass and radius [4]. In addition, quarks would alter  $\nu$  emissivities and thereby influence the surface temperature of a neutron star [5] during the hundreds of thousands or millions of years that they might remain observable with such instruments as HST, Chandra, and XMM. Quarks would also alter the spin-down rates of neutron stars [6].

Many calculations of dense matter predict the appearance of other kinds of exotic matter in addition to quarks: for example, hyperons or a Bose (pion, kaon) condensate (cf. [7] and references therein). An important issue is whether or not  $\nu$  observations from a supernova could reveal the presence of such exotic matter and, further, could unambiguously point to the appearance of quarks. The detection of quarks in neutron stars would go a long way toward the delineation of QCD at finite baryon density which would be complementary to current relativistic heavy ion collider experiments, which largely address the finite temperature, but baryon-poor regime.

An important consequence of the existence of exotic matter in neutron stars (in whatever form, as long as it contains a negatively charged component) is that a sufficiently massive PNS becomes metastable [8]. After a delay

of up to 100 s, depending upon which component appears, a metastable PNS collapses into a black hole [9–11]. The collapse to a black hole proceeds on a free-fall time scale of less than a millisecond [12], much shorter than  $\nu$  diffusion times, and the neutrinos still trapped in the inner regions cannot escape. Such an event should be straightforward to observe as an abrupt cessation of  $\nu$  flux when the instability is triggered [13].

The evolution of the PNS in the so-called Kelvin-Helmholtz phase, during which the remnant changes from a hot,  $\nu$ -trapped, and lepton-rich object to a cold and  $\nu$ -free star, occurs in near-hydrostatic equilibrium. The  $\nu$ -matter interaction time scales are much smaller than the dynamical time scale of PNS evolution, which is of the order of seconds. Thus, until neutrinos enter the semitransparent region at the edge of the star, they remain close to thermal equilibrium with matter and may be treated in the diffusion approximation.

In this Letter we provide a benchmark calculation with quarks by solving the general relativistic  $\nu$  transport and hydrostatic equations (as in [10]) and then compare our results with those of our previous work [10,11] in which other compositions were studied. In addition, we assess the prospects of observing PNS metastability and its subsequent collapse to a black hole through observations in current and planned detectors.

The essential microphysical ingredients in our study are the EOS of dense matter and its associated  $\nu$  opacity. We begin by considering two generic compositions: charge-neutral, beta equilibrated matter containing (i) nucleons only ( $np$ ) and (ii) nucleons with quark matter ( $npQ$ ). In the  $npQ$  case, a mixed phase of baryons and quarks (pure quark matter exists only for very large baryon densities, except for extreme choices of model parameters) is constructed by satisfying Gibbs' phase rules for mechanical, chemical, and thermal equilibrium [14]. The EOS of baryonic matter is calculated using a field-theoretic model at the mean field level [15]. The results reported with this EOS are quite general, as we verified by alternatively using a potential model approach [7]. The quark matter EOS is calculated using a MIT baglike model (similar results are obtained with the Nambu–Jona-Lasinio quark model).

The details of the EOS may be found in Ref. [16]. We use  $\nu$  opacities [17,18] consistent with the EOS. When quarks appear, the  $\nu$  absorption and scattering cross sections dramatically decrease, the precise reduction being sensitive to the thermodynamic conditions in the mixed phase [18].

Figure 1 shows the evolutions of some thermodynamic quantities at the center of  $npQ$  stars of various, fixed, baryonic masses ( $M_B$ ). In the absence of accretion,  $M_B$  remains constant during the evolution, while the gravitational mass  $M_G$  decreases. With the EOS utilized, stars with  $M_B \leq 1.1M_\odot$  do not contain quarks and those with  $M_B \geq 1.7M_\odot$  are metastable. The latter value is  $\sim 0.05M_\odot$  larger than the maximum mass for cold, catalyzed  $npQ$  matter, because the maximum mass of hot  $\nu$ -free  $npQ$  matter is this much less than that of hot  $\nu$ -trapped matter [18]. Generally, due to the high lepton ( $\nu$ ) content initially present in the PNS, the electron chemical potential at the center is too large for quarks to exist. For sufficiently massive stars, quarks eventually appear after a certain amount of  $\nu$  loss occurs. For the  $M_B = 1.6M_\odot$  star, for example, quarks appear after about 15 s (indicated by a diamond). Thereafter, the star's central density increases for a further 15–20 s, until a new stationary state with a quark-hadron mixed phase core is reached (for stable stars) or for  $M_B \geq 1.7M_\odot$ , instability occurs (indicated by asterisks). It is interesting that for this EOS the lifetimes for all masses are restricted to the range 10–30 s, and slowly decrease with increasing mass. The appearance of quarks is accompanied by an

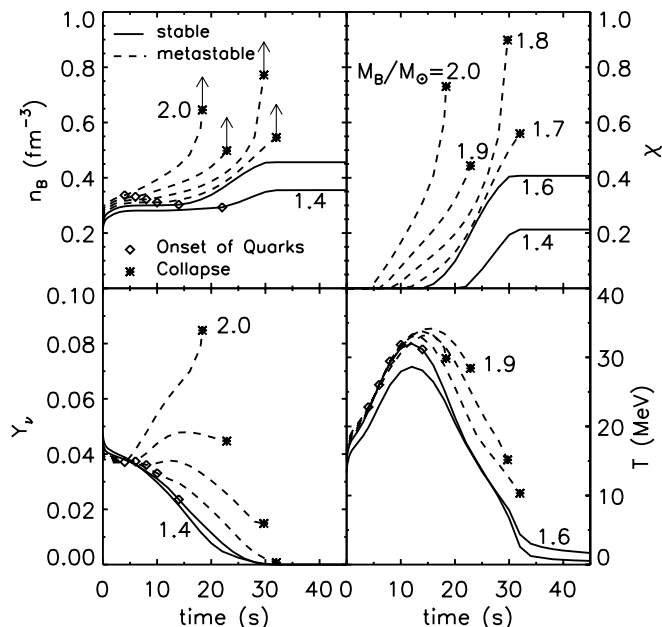


FIG. 1. Evolutions of the central baryon density  $n_B$ ,  $\nu$  concentration  $Y_\nu$ , quark volume fraction  $\chi$ , and temperature  $T$  for different baryonic masses  $M_B$ . Solid lines correspond to stable stars; stars with larger masses are metastable (dashed lines). Diamonds indicate when quarks appear at the star's center, and asterisks denote when metastable stars become gravitationally unstable.

increase in  $Y_\nu$  because of the depletion of electrons; for the largest masses, the increase is very large.

To point out the major differences one might observe between the  $np$  and  $npQ$  cases, we have estimated the  $\bar{\nu}_e$  count rate in the Super-K detector in Fig. 2. For this estimate, we assumed the total  $\nu$  luminosity from a PNS at 8.5 kpc distance, corresponding to a Galactic supernova, was equally divided among the six  $\nu$  species. The  $\nu$ -energy spectra were taken to be Fermi-Dirac with zero chemical potential and a temperature corresponding to the matter temperature in the PNS where the  $\nu$ -optical depth was approximately unity. Only the dominant reaction,  $\bar{\nu}_e$  absorption on protons, was included. (For details, see [11].) It is difficult to discern much difference in the early ( $t < 10$  s) count rates from  $np$  and  $npQ$  stars. For stars with  $M_B < 1.7M_\odot$ , this is because quarks have not yet appeared. For more massive stars, the fact that neutrinos are strongly trapped inhibits any discriminatory signal from reaching the surface before this time. The signals at later times ( $t \geq 25$  s), however, are substantially larger for the  $npQ$  case, due to the decrease in  $\nu$  opacity of  $npQ$  matter and the increased binding energy of  $npQ$  stars. Most importantly, the  $\nu$  signal from metastable  $npQ$  stars halts abruptly when the instability occurs. Qualitatively, these features are also found for  $npH$  and  $npK$  stars [10,11].

We compare  $\nu$  signals observable with different detectors in Fig. 3, which displays the  $\nu$ -light curves as a function of  $M_B$  for  $npQ$  stars. The two upper shaded bands correspond to estimated SN 1987A (50 kpc distance) detection limits with KII and IMB, and the lower bands correspond to estimated detection limits in SNO, Super-K, and UNO, for a Galactic supernova (8.5 kpc distance). The detection limits have been set to a  $\bar{\nu}_e$  count rate  $dN/dt = 0.2$  Hz [11] with the same assumptions as in Fig. 2. The general rise with time of the detector limits is chiefly due to the steady decrease in the  $\bar{\nu}_e$  average energy. It is possible that these limits are too conservative

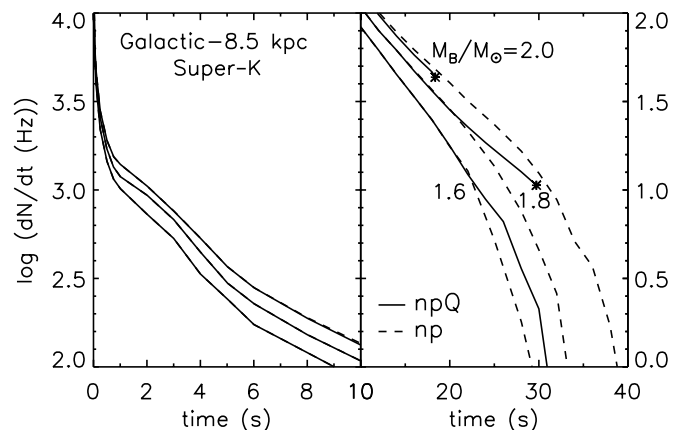


FIG. 2. A comparison of  $\bar{\nu}_e$  count rates expected in Super-K from a PNS containing either  $np$  or  $npQ$  matter. The left panel shows times less than 10 s, while the right panel shows times greater than 10 s.

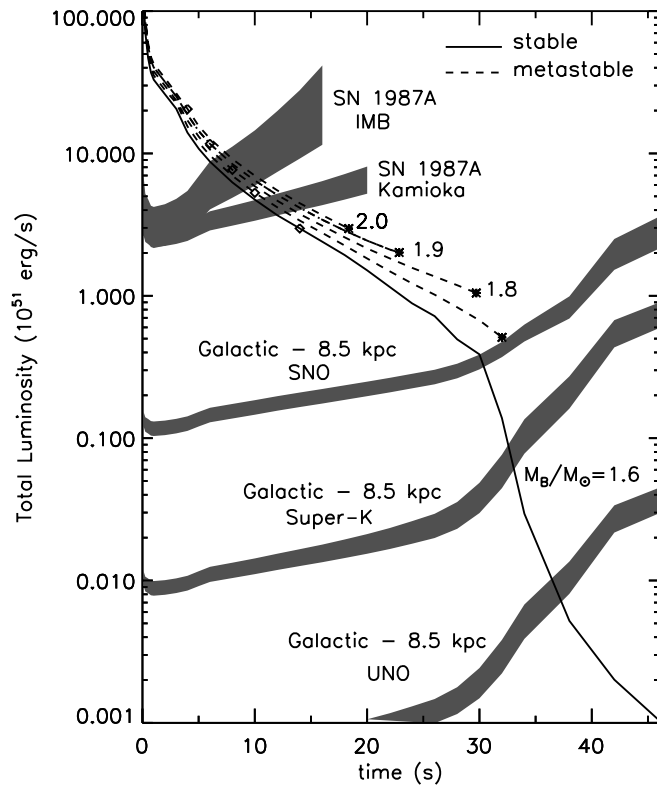


FIG. 3. The total  $\nu$  luminosity for  $npQ$  stars of various baryon masses. Shaded bands illustrate the limiting luminosities corresponding to count rates of 0.2 Hz for the indicated supernovae in some detectors.

and could be lowered with identifiable backgrounds and knowledge of the direction of the signal. The width of the bands represents the uncertainty in the  $\bar{\nu}_e$  average energy due to the flux-limited diffusion approximation. We conclude that it should be possible to distinguish between stable and metastable stars, since the luminosities when metastability is reached are always above conservative detection limits.

The drop in  $\nu$  luminosity for stable stars is associated with the end of the Kelvin-Helmholtz epoch when the PNS is becoming optically thin. This portion of the  $\nu$ -light curve is approximate due to the breakdown of the diffusion approximation. It is an apparent coincidence that this occurs simultaneously with the collapse of the lower mass metastable stars.

Our choice of bag constant,  $B = 150 \text{ MeV fm}^{-3}$ , in conjunction with the baryonic EOS we used, was motivated to maximize the extent of the quark matter phase in a cold neutron star and was limited by the necessity of producing a maximum mass cold star in line with accurate observational constraints ( $M_G = 1.444M_\odot$  [19]). Increasing  $B$ , or employing an alternative quark EOS that otherwise produces a larger maximum mass, delays the appearance of quarks and raises the metastability window to larger stellar masses. Necessarily, this results in an increased time scale for metastability for a given mass, and

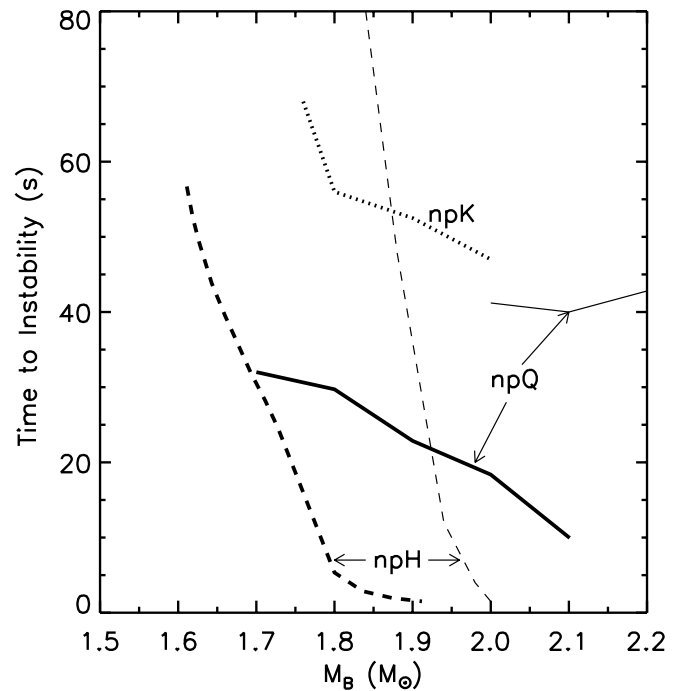


FIG. 4. Lifetimes of metastable stars versus the PNS  $M_B$  for various assumed compositions. Thick lines denote cases in which the maximum masses of cold, catalyzed stars are near  $M_G \approx 1.45M_\odot$ , which minimizes the metastability lifetimes. The thin lines for the  $npQ$  and  $npH$  cases are for EOSs with larger maximum masses ( $M_G = 1.85M_\odot$  and  $1.55M_\odot$ , respectively.)

a lower  $\nu$  luminosity when metastability occurs. Figure 4 shows the relation between time to instability and  $M_B$  for the original case ( $B = 150 \text{ MeV fm}^{-3}$ , thick solid curve) and a case with  $B = 200 \text{ MeV fm}^{-3}$  (thin solid curve), in which the maximum gravitational mass of a cold neutron star is about  $1.85M_\odot$ . For the latter case, the metastability time scales lie in a narrow range 40–45 s. These, and the metastability masses, are both larger than obtained for  $B = 150 \text{ MeV fm}^{-3}$  and have narrower ranges. Further increases in  $B$  diminish the size of the instability window, because the appearance of quarks is shifted to progressively larger densities.

Figure 4 also compares the metastability time- $M_B$  relation found for matter containing hyperons ( $npH$ , dashed lines [10]) or matter with kaons ( $npK$ , dotted line [11]) instead of quarks. All three types of strange matter are suppressed by trapped neutrinos [7,16], but hyperons always exist in  $npH$  matter at finite temperatures and the transition to quark matter can occur at lower densities than that for very optimistic kaon cases [11]. Thus, the metastability time scales for  $npH$  matter can be very short, and those for  $npK$  matter are generally larger than for  $npQ$  matter. Note the relatively steep dependence of the metastability time with  $M_B$  for  $npH$  stars, which decreases to very small values near the maximum mass limit of hot, lepton-rich, stars. The thick  $npH$  and  $npQ$  lines, as well as the  $npK$  line, represent minimum metastability times for a given

$M_B$  as discussed above. The thin  $npQ$  and  $npH$  lines are for EOSs with larger cold, catalyzed maximum mass.

Clearly, the observation of a single case of metastability, and the determination of the metastability time alone, will not necessarily permit one to distinguish among the various possibilities. Only if the metastability time is less than 10–15 s could one decide on this basis that the star's composition was that of  $npH$  matter. However, as in the case of SN 1987A, independent estimates of  $M_B$  might be available [20]. In addition, the observation of two or more metastable neutron stars might permit one to differentiate among these models, but given the estimated rate of Galactic supernova (one per 30–50 yr [21]), this may prove time-consuming.

Our study has focused on times longer than approximately 1 s after core bounce, after which effects of dynamics and accretion become unimportant. Studies of the  $\nu$  signal during the first second, during which approximately 1/3 of the energy is emitted, and at late times, as the star becomes optically thin to neutrinos, requires more accurate techniques for  $\nu$  transport. In addition, the earliest time periods require the incorporation of hydrodynamics [22].

Our conclusions are that (1) the metastability and subsequent collapse to a black hole of a PNS containing quark matter, or other types of matter including hyperons or a Bose condensate, are observable in current and planned  $\nu$  detectors and (2) discriminating among these compositions may require more than one such observation. This highlights the need for breakthroughs in lattice simulations of QCD at finite baryon density to unambiguously determine the EOS of high density matter. In the meantime, intriguing possible extensions of PNS simulations with  $npQ$  matter include the consideration of heterogeneous structures [23], quark matter superfluidity [24], and coherent  $\nu$  scattering on droplets [25].

This work was supported by U.S. Department of Energy Grants No. DOE/DE-FG02-87ER-40317 and No. DOE/DE-FG02-88ER-40388. J. A. P. acknowledges J. A. Miralles for interesting discussions.

- 
- [1] A. Burrows and J. M. Lattimer, *Astrophys. J.* **307**, 178 (1986).  
 [2] C. K. Jung, in *Next Generation Nucleon Decay and Neutrino Detector*, edited by M. V. Diwan and C. K. Jung, AIP Conf. Proc. No. 533 (AIP, New York, 2000), p. 29.  
 [3] J. C. Collins and M. J. Perry, *Phys. Rev. Lett.* **34**, 1353 (1975).

- [4] J. M. Lattimer and M. Prakash, *Astrophys. J.* **550**, 426 (2001).  
 [5] D. Page, M. Prakash, J. M. Lattimer, and A. W. Steiner, *Phys. Rev. Lett.* **85**, 2048 (2000).  
 [6] N. K. Glendenning, S. Pei, and F. Weber, *Phys. Rev. Lett.* **79**, 1603 (1997).  
 [7] M. Prakash *et al.*, *Phys. Rep.* **280**, 1 (1997).  
 [8] V. Thorsson, M. Prakash, and J. M. Lattimer, *Nucl. Phys.* **A572**, 693 (1994); G. E. Brown, *Nucl. Phys.* **A574**, 217 (1994); G. E. Brown and H. A. Bethe, *Astrophys. J.* **423**, 659 (1994); M. Prakash, J. Cooke, and J. M. Lattimer, *Phys. Rev. D* **52**, 661 (1995); N. K. Glendenning, *Astrophys. J.* **448**, 797 (1995); P. J. Ellis, J. M. Lattimer, and M. Prakash, *Comments Nucl. Part. Phys.* **22**, 63 (1996); I. Bombaci, *Astron. Astrophys.* **305**, 871 (1996).  
 [9] W. Keil and H-Th. Janka, *Astron. Astrophys.* **296**, 145 (1995).  
 [10] J. A. Pons, S. Reddy, M. Prakash, J. M. Lattimer, and J. A. Miralles, *Astrophys. J.* **513**, 780 (1999).  
 [11] J. A. Pons, J. A. Miralles, M. Prakash, and J. M. Lattimer, *Astrophys. J.* **553**, 382 (2001).  
 [12] T. W. Baumgarte, S. L. Shapiro, and T. A. Teukolsky, *Astrophys. J.* **458**, 680 (1996); J. A. Pons, Ph.D. thesis, University of Valencia, 1999.  
 [13] A. Burrows, *Astrophys. J.* **334**, 897 (1988); although done for a rapid accretion-induced collapse, his discussion applies also to the present case in which collapse occurs on the much longer deleptonization time scale of 10–60 s.  
 [14] N. K. Glendenning, *Phys. Rev. D* **46**, 1274 (1992).  
 [15] H. Müller and B. D. Serot, *Nucl. Phys.* **A606**, 508 (1996).  
 [16] A. W. Steiner, M. Prakash, and J. M. Lattimer, *Phys. Lett. B* **486**, 239 (2000).  
 [17] S. Reddy, M. Prakash, and J. M. Lattimer, *Phys. Rev. D* **58**, 013009 (1998).  
 [18] A. W. Steiner, M. Prakash, and J. M. Lattimer, astro-ph/0101566 [*Phys. Lett. B* (to be published)].  
 [19] S. E. Thorsett and D. Chakrabarty, *Astrophys. J.* **512**, 288 (1999).  
 [20] F.-K. Thielemann, M. Hashimoto, and K. Nomoto, *Astrophys. J.* **349**, 22 (1990); H. A. Bethe and G. E. Brown, *Astrophys. J. Lett.* **445**, L29 (1995).  
 [21] S. van den Bergh and G. A. Tammann, *Annu. Rev. Astron. Astrophys.* **29**, 363 (1991); E. Cappellaro, R. Evans, and M. Turatto, *Astron. Astrophys.* **351**, 459 (1999).  
 [22] O. E. B. Messer *et al.*, *Astrophys. J.* **507**, 353 (1998); S. Yamada, H-Th. Janka, and H. Suzuki, *Astron. Astrophys.* **344**, 533 (1999); A. Burrows *et al.*, *Astrophys. J.* **539**, 865 (2000); M. Rampp and H-Th. Janka, *Astrophys. J.* **539**, L33 (2000); M. Liebendoerfer *et al.*, *Phys. Rev. D* **63**, 103004 (2001).  
 [23] M. B. Christiansen, N. K. Glendenning, and J. Schaffner-Bielich, *Phys. Rev. C* **62**, 025804 (2000).  
 [24] G. W. Carter and S. Reddy, *Phys. Rev. D* **62**, 103002 (2000).  
 [25] S. Reddy, G. Bertsch, and M. Prakash, *Phys. Lett. B* **475**, 1 (2000).